Reut and Beck columns: effects of end gravity force, translational and rotational inertias

Columnas de Beck y Reut: efectos de una fuerza de gravedad en el borde libre, inercias traslacionales y rotacionales

Luis G. Arboleda Monsalve[1], *David G. Zapata Medina*[1*], *J. Darío Aristizabal Ochoa*[2]

[1]Dept. of Civil and Environmental Engineering, Northwestern Univ. 2145 Sheridan Rd. Room A236. Evanston, IL 60208. United States of America.

[2]School of Mines, National University of Colombia. Cra 80 Nº 65-223. Medellín, Colombia.

(Recibido el 24 de agosto de 2012. Aceptado el 6 de noviembre de 2012)

Abstract

The stability of Reut and Beck columns subjected to any combination of gravity and non-conservative (fixed-line or follower) compressive axial forces is presented using the dynamic formulation. The proposed method is general capturing the static (or divergence) buckling as well as the dynamic (flutter) instability of cantilever columns. Special attention is given to the effects of the end gravity force, translational and rotational inertias along the member. Analytical results are intended to capture the limit on the range of applicability of the static or Euler's method in the stability analysis of slender cantilever columns, and to define the transition from static instability (with zero frequency) to dynamic instability ("flutter"). Finally, the comparison between the characteristic stability equations of slender Reut and Beck columns is presented.

--------- *Keywords:* Columns, buckling, dynamic stability, static stability, flutter, non-conservative loads, Beck and Reut columns

Resumen

Se presenta la estabilidad de las columnas de Reut y Beck sometidas a cualquier combinación de fuerzas compresivas axiales de gravedad y no conservativas (fuerza fija a lo largo de una línea o seguidora) utilizando la

* Autor de correspondencia: teléfono: + 1 + 773 + 209-4554, fax: + 1 + 847 + 491-4011, correo electrónico: zapata@u.northwestern.edu (D. Zapata)

formulación dinámica. El método propuesto es general y captura el pandeo estático (o divergencia) y la inestabilidad dinámica ("flameo") de columnas en voladizo. Los efectos de la fuerza de gravedad y las inercias traslacionales y rotacionales a lo largo del elemento se analizan cuidadosamente. También se presentan resultados analíticos que capturan el límite del rango de aplicabilidad del método estático o de Euler en el análisis de estabilidad de columnas esbeltas en voladizo y la transición de inestabilidad estática (con frecuencia cero) a inestabilidad dinámica ("flameo"). Finalmente se presenta la comparación entre las ecuaciones características de estabilidad de columnas esbeltas de Reut y Beck.

---------- *Palabras clave:* Columnas, pandeo, estabilidad dinámica, estabilidad estática, flameo, fuerzas no conservativas, columnas de Beck y Reut.

Introduction

The static and dynamic stabilities of slender beam-columns subjected to non-conservative end loads like those produced by jet engines or rockets and cantilevered pipes conveying fluid are of great importance in mechanical, aeronautical, structural and aerospace engineering. The problem of follower forces on slender columns has been the main subject of many textbooks such as those by [1-3]. It has also been presented in several state-of-art review papers such as those by [4-6]. The stability problem has also been verified experimentally by [7, 8] while numerical verifications using the finite element program LS-DYNA were presented by [9]. This topic has been extensively studied by numerous researchers from different points of view, but due to space limitations just a few of them are presented herein. For instance, [10] studied the stability of a clamped-elastically restrained column subjected to a partially follower force using the Timoshenko approach. [11] studied the instability of a cantilever beam and a simply supported plate under both conservative and non-conservative loads. [12] presented an algorithm to determine the free vibration frequencies of beams subjected to conservative and non-conservative static loads. [13] studied the effects of an elastic Winkler and rotatory foundations on the stability of a pipe conveying fluid. [14] discussed several non-classical stability problems of cantilever columns filled with liquid or subjected to gas pressure and the applicability of the dynamic stability method.

The post-buckling behavior of the Beck column was presented by [15] showing the effect of a tip mass with rotatory inertia. [16] studied the effects of an elastic foundation on the Beck column. [17] presented experimental and theoretical results and the effects of lumped external damping on the dynamic stability of the Beck column. [18] investigated the effect of a single crack on the divergence buckling and flutter of a column subjected to a triangularly sub-tangential force. [19] developed the stability equations of the generalized Euler column showing the range of applicability of the static approach on non-conservative problems. Recently, [20] studied the influence of an attached end mass on the static and dynamic stability of an elastically restrained Beck column.

The main objective of this publication is to present the closed-form eigenvalue equation for the dynamic stability of both Reut and Beck columns including the effects of an axial gravity load applied at the top end, and the translational and rotatory inertias of the column itself. A sensitivity study is carried out showing the transition from static instability (with zero frequency) to dynamic instability and the interactions between the seven input parameters.

Structural model

Consider a prismatic element that connects points A (perfectly clamped end) and B (free end), see figure 1. It is assumed that: 1) the beam-column AB is made of a homogenous linear elastic material with modulus E; 2) its centroidal axis is a straight line; 3) is subjected to a combination of a gravity axial force P_0, and a non-conservative axial force P_f, applied at the free end B; 4) its transverse cross section is doubly symmetric with a total area A, principal moment of inertia I about its plane of bending, and uniform mass per unit of length $\overline{m}$, with a radius of gyration r; and 5) all transverse deflections, rotations, and strains along the beam are small, so that the principle of superposition is applicable.

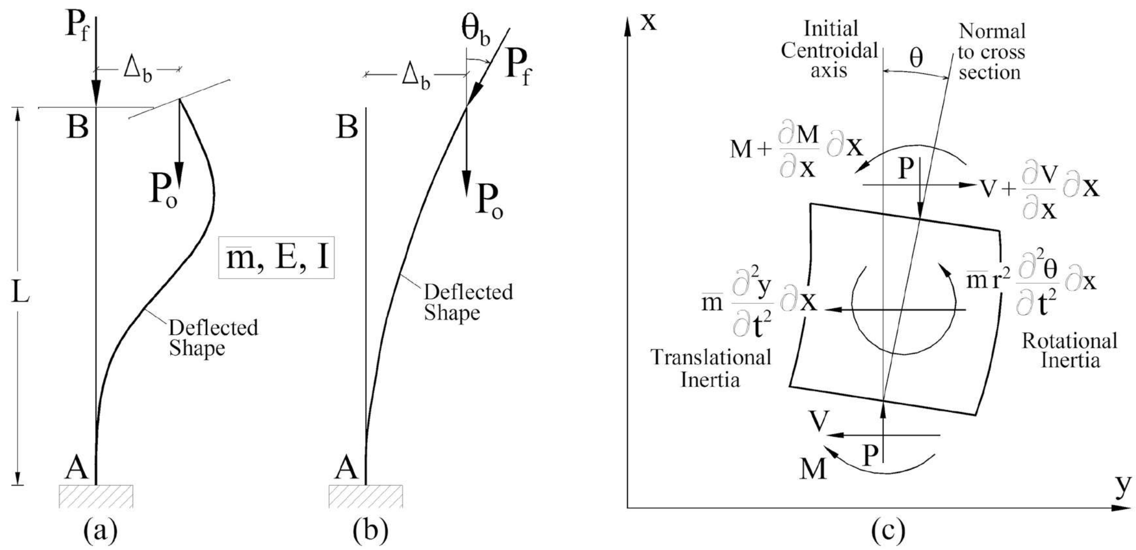

Figure 1 Structural model of cantilever column under gravity and non-conservative forces: (a) Reut column; (b) Beck column; and (c) differential element (forces, moments and deformations)

Governing equations and general solution

The transverse and bending equilibrium equations of the differential element shown in figure 1(c) are:

$$\frac{\partial V}{\partial x} = \overline{m}\frac{\partial^2 y}{\partial t^2} \tag{1}$$

$$\frac{\partial M}{\partial x} = V + P\frac{\partial y}{\partial x} - \overline{m}r^2\frac{\partial^2 \theta}{\partial t^2} \tag{2}$$

Knowing that: $M = EI(\partial^2 y / \partial x^2)$, $\theta = \partial y / \partial x$ and substituting (1) into (2) after differentiation, the following equation in terms of y can be obtained:

$$EI\frac{\partial^4 y}{\partial x^4} + P\frac{\partial^2 y}{\partial x^2} + \overline{m}\frac{\partial^2 y}{\partial t^2} - \overline{m}r^2\frac{\partial^2}{\partial t^2}\left(\frac{\partial^2 y}{\partial x^2}\right) = 0 \tag{3}$$

Assuming exponential variations of the bending deflection [i.e., $y(x, t) = Y(x)e^{iwt}$, with Y representing the shape function associated with the lateral deflection along the member] and substituting into Eq. (3), the differential equations adopts the form:

$$\frac{d^4 Y}{dx^4} + \frac{\phi^2}{L^2}\frac{d^2 Y}{dx^2} - \frac{T_I}{L^4}Y = 0 \tag{4}$$

where:

$$\phi^2 = PL^2/EI + R_I^2 \tag{5}$$

$$R_I^2 = \overline{m}\omega^2 r^2 L^2/EI \tag{6}$$

$$T_I^2 = \overline{m}\omega^2 L^4/EI \tag{7}$$

$$P = P_0 + P_f = \phi^2 EI/L^2 - \overline{m}\omega^2 r^2 \tag{8}$$

Eqs. (6-8) are the rotational inertia, translational inertia and non-conservative/gravity force parameters, respectively.

Eq. (8) was also used by [19] for the particular case of ω = 0 (static stability). Notice that the net effect of the rotatory inertia is to reduce the total axial load capacity of the column. The solution to Eq. (4), which is a linear fourth-order homogeneous differential equation, is of the form:

$$Y(x) = ce^{mx} \tag{9}$$

After substituting Eq. (9) into the governing Eq. (4), a fourth-degree polynomial is obtained:

$$m^4 + \frac{\phi^2}{L^2}m^2 - \frac{T_I^2}{L^4} = 0 \tag{10}$$

whose solutions are:

$$m = \pm i\lambda/L;\ \pm\alpha/L \tag{11}$$

where:

$$\lambda = \sqrt{\phi^2/2 + \sqrt{\phi^4/4 + T_I^2}} \tag{12}$$

$$\alpha = \sqrt{-\phi^2/2 + \sqrt{\phi^4/4 + T_I^2}} \tag{13}$$

Therefore, the solution for Y is:

$$\begin{aligned} Y(x) &= C_1 \sin(\lambda x/L) + C_2 \cos(\lambda x/L) \\ &+ C_3 \sinh(\alpha x/L) + C_4 \cosh(\alpha x/L) \end{aligned} \tag{14}$$

Once Eq. (14) is obtained, the bending slope, Θ, shear force, V, and bending moment, M, along the member can be obtained as follows:

$$\begin{aligned} \Theta(x) &= C_1\frac{\lambda}{L}\cos\left(\frac{\lambda x}{L}\right) - C_2\frac{\lambda}{L}\sin\left(\frac{\lambda x}{L}\right) \\ &+C_3\frac{\alpha}{L}\cosh\left(\frac{\alpha x}{L}\right) + C_4\frac{\alpha}{L}\sinh\left(\frac{\alpha x}{L}\right) \end{aligned} \tag{15}$$

$$\begin{aligned} V(x) = \frac{EI}{L^2}\Bigg[& C_1\frac{\lambda\alpha^2}{L}\cos\left(\frac{\lambda x}{L}\right) - C_2\frac{\lambda\alpha^2}{L}\sin\left(\frac{\lambda x}{L}\right) \\ & - C_3\frac{\alpha\lambda^2}{L}\cosh\left(\frac{\alpha x}{L}\right) - C_4\frac{\alpha\lambda^2}{L}\sinh\left(\frac{\alpha x}{L}\right)\Bigg] \end{aligned} \tag{16}$$

$$\begin{aligned} M(x) = \frac{EI}{L}\Bigg[& C_1\frac{\lambda^2}{L}\sin\left(\frac{\lambda x}{L}\right) + C_2\frac{\lambda^2}{L}\cos\left(\frac{\lambda x}{L}\right) \\ & - C_3\frac{\alpha^2}{L}\sinh\left(\frac{\alpha x}{L}\right) - C_4\frac{\alpha^2}{L}\cosh\left(\frac{\alpha x}{L}\right)\Bigg] \end{aligned} \tag{17}$$

Eqs. (14-17) are given in terms of four constants C_1, C_2, C_3 and C_4 which must be determined using four boundary conditions as described next.

Dynamic stability of a cantilever column subjected to gravity and fixed-line forces

The boundary conditions of the column of figure 1(a) are:

At $x = 0$: $Y(0) = 0$; and $\Theta(0) = 0$

At $x = L$: $V(L) = 0$; and $M(L) = (P_f/P)(\phi^2 - R_I^2)Y(L)$

Using Eqs. (14-17) and the four boundary conditions just described, the following characteristic equation for the dynamic stability of the column of figure 1(a) is obtained:

$$\begin{aligned} &(\alpha^4 + \lambda^4)cos\lambda cosh\alpha + 2T_I^2 - T_I\phi^2 sin\lambda sinh\alpha \\ &\quad + (P_f/P)(\phi^2 - R_I^2) \\ &[\phi^2(1 - cos\lambda cosh\alpha) + 2T_I sin\lambda sinh\alpha] = 0 \end{aligned} \tag{18}$$

Eq. (18) indicates that the dynamic stability of a cantilever column subjected to combined gravity and non-conservative force depends on seven variables: $\overline{m}$, r, ω, L, E, P_f and P_0. On the other hand, the static stability equation for this particular case can be obtained by making $R_I = T_I = 0$. Then, Eqs. (12) and (13) become ϕ and zero, respectively, and the static stability equation becomes:

$$cos\phi = -P_f/P_0 \tag{19}$$

Eq. (19) is identical to those proposed by [1] (p. 103) and by [19].

Dynamic stability of a cantilever column subjected to gravity and follower forces

The boundary conditions of the column shown in figure 1(b) are:

At $x = 0$: $Y(0) = 0$; and $\Theta(0) = 0$

At $x = L$: $V(L) = -(P_f/P)(\phi^2 - R_f^2)\theta(L)$; and $M(L) = 0$

Using Eqs. (14-17) and the four boundary conditions just described, the characteristic equation for the dynamic stability of the column of figure 1(b) is found to be identical to Eq. (18). Consequently, the dynamic stability of the Beck column corresponds also to the Reut column.

Effects of gravity load, translational and rotational inertias on the dynamic stability of reut and beck columns

Variations of the total buckling load $P = P_0 + P_f$ with the ratio P_f / P_0, the natural frequency ω and the ratio r/L were calculated and plotted using Eq. (18). Figures 2, 3 and 4 show the influence of the gravity load, translational and rotational inertias on the buckling loads of both columns of figures 1(a) and 1(b). Note on figures 2(a-g) that the vertical axis shows the total buckling load P normalized with respect to the Euler load $P^* = \pi^2 EI/(4L^2)$ versus the corresponding natural frequency normalized with respect to $\omega^* = (1.875)^2\sqrt{EI/(\bar{m}L^4)}$ along the horizontal axis for different values of P_f/P_0 and r/L, respectively (where ω^* is the first natural frequency of the member as a cantilever beam with $P_0 = P_f = r/L = 0$). In figures 2(a-g) the ratio P_f/P_0 varies from zero (i.e., $P_f = 0$ corresponding to the Euler column with only gravity load P_0 being applied) to infinity (i.e., $P_0 = 0$ with only P_f being applied corresponding to Reut and Beck columns) for seven different values of r/L (= 0, 0.15, 0.30, 0.50, 0.57, 0.75 and 1, respectively). Values of $r/L < 0.15$ represent common reinforced-concrete members. Higher values of r/L can be obtained for short elements as in the case of columns weakened by the development of a plastic hinge during an earthquake, bridge piers deteriorated by a collision, and gusset plates exposed to pack rust or pitting [21]. Depending on the column material and cross section geometry, special care is needed for these column cases as shear deformations become significant.

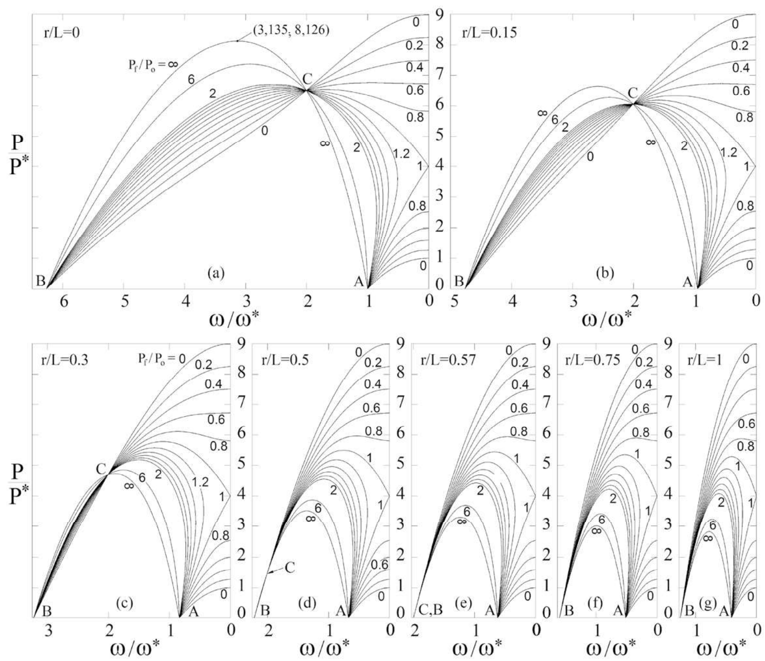

Figure 2 Variations of P / P^* with ω/ω^* for different values of P_f / P_0 and *r/L*

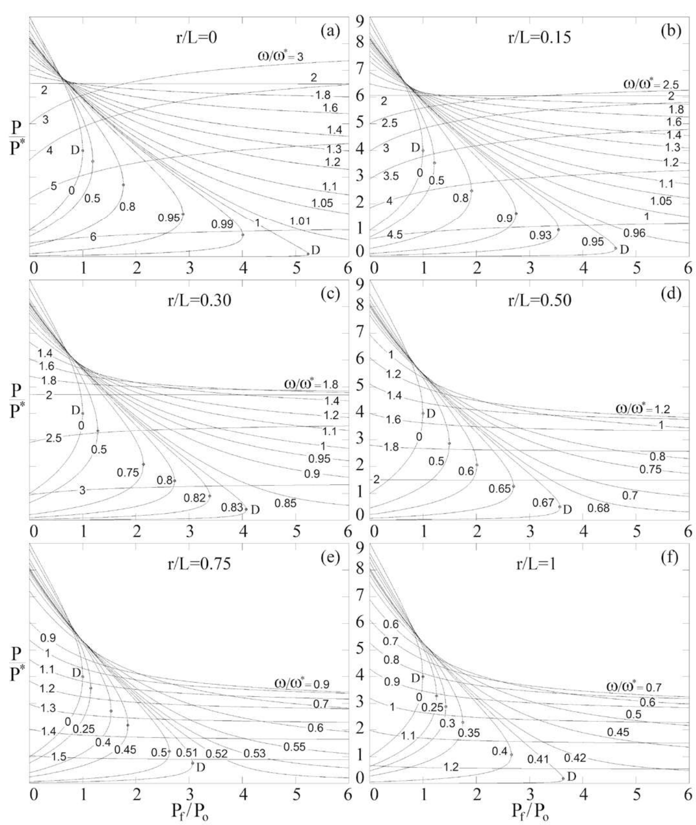

Figure 3 Variations of P / P^* with P_f / P_0 for different values of ω/ω^* and *r/L*

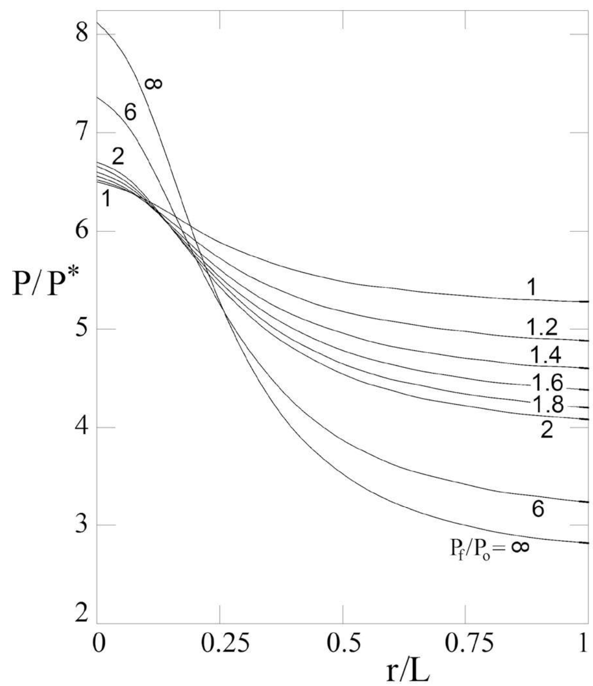

Figure 4 Variation of the peak value of P / P^* (at Flutter) with *r/L* for different values of P_f / P_0

Figures 3(a-f) show the variation of P / P^* with the ratio P_f / P_0 for different values of ω/ω^* and for six different cases of *r/L* (= 0, 0.15, 0.30, 0.50, 0.75 and 1, respectively). The set of Figures 2 and 3 represent the traces or curves on the (P / P^*, ω/ω^*) and (P / P^*, P_f / P_0) planes of the surfaces generated by Eq. (18) in a 3D orthogonal system of axis P / P^*, P_f / P_0 and ω/ω^*, respectively, for different values of *r/L*.

Figure 4 shows the variation of the maximum axial load $P = P_0 + P_f$ (when the phenomenon of flutter starts to occur) with the ratio *r/L* for eight different values of P_f / P_0 (= 1.01, 1.20, 1.40, 1.60, 1.80, 2, 6 and ∞, respectively). The maximum axial load *P*, which corresponds to the peaks of the curves shown in figures. 2(a-g), is normalized with respect to the classical Euler load $P^* = \pi^2 EI/(4L^2)$. Each peak in the curves of figures 2(a-g) corresponds to the phenomenon of flutter when the natural frequencies of the first and second modes of vibration become identical to each other.

Based on the curves shown in figures 2, 3 and 4, the following conclusions can be drawn:

The intersections of the curves with the horizontal axis ω/ω^* indicated by points A and B in figures 2(a-g) represent the natural frequencies corresponding to the first and second mode of vibration of a cantilever beam (with $P_0 = P_f = 0$). For example, figure 2(a) indicates that for $r/L = 0$: $\omega_1 = \omega^* = (1.875)^2\sqrt{EI/(\bar{m}L^4)}$ and $\omega^2 = 6.267\omega^*$ which are identical to those reported in the technical literature [22, 23]. Figure 2(g) shows that for $r/L = 1$ the natural frequencies are $\omega_1 = 0.410\ \omega^*$ and $\omega_2 = 1.249\ \omega^*$. Those values represent reductions of 59% and 80% in the first and second natural frequencies in perfectly clamped cantilever beams when the radius of gyration is increased from zero to *L*.

The vertical axis P/P^* in figures 2(a-g) represent the static buckling loads (i.e., $\omega = 0$) of the member and, as expected, these are not affected by the ratio *r/L* . For example, figures 2(a-g) indicate that for $P_f / P_0 = 0$: $P_1 = P^* = \pi^2 EI/(4L^2)$ and $P_1 = 9P^*$ which are identical to those reported in technical literature for cantilever columns subjected to gravity load only [24]. The intersections of the curves with the vertical P/P^* axis for the cases of static buckling when $0 < P_f / P_0 < 1$ can be obtained from Eq. (19).

Figures 2(a-g) indicate that for $0 < P_f/P_0 < 1$, the axial load *P* reduces the natural frequencies, and the presence of the non-conservative force P_f has a stabilizing effect increasing the buckling load *P* as claimed by [2] (p. 103). Note that in the range $0 < \omega/\omega^* < 0.25$ and for $0 < P_f / P_0 < 0.8$, both inertias (translational and rotational) have little effect on the load capacity *P*. However, when $P_f / P_0 > 0.8$ the load capacity *P* is highly affected by both inertias.

Figures 2(a-g) also indicates that: a) the transition from static instability to dynamic instability occurs for $P_f / P_0 = 1$ when the critical loads corresponding to the first and second buckling mode become identical to each other $P_1 = P_2 = P^* = \pi^2 EI/L^2$). This feature was fully discussed by [19]; b) for $P_f / P_0 > 1$, the column reaches a state of dynamic instability (i.e., with $\omega > 0$) with the buckling load depending on the inertias (both translational and rotational); and c) flutter starts to take place only when $P_f / P_0 > 1$ at an axial load P corresponding to the peaks of the curves in figures 2(a-g) and the natural frequencies of the first and second modes of vibration of the member become identical to each other. For instance, flutter occurs at $\omega/\omega^* = 3.135$ and $P / P^* = 8.126$ as indicated by such peak corresponding to $r/L = 0$ and $P_f / P_0 = \infty$ in figure 2(a). [24] (p. 155) reported identical values for this particular case. The value of $P = 8.126P^* = 20.05EI / L^2$ was also reported by [1]. Notice that the load and frequency at which flutter occurs are reduced as r / L increases.

An interesting feature shown by all curves in figures 2(a-e) with $P_f / P_0 > 1$ is the common point C which occurs exactly at $\omega/\omega^* = 2$ with the corresponding value of P/P^* decreasing as r/L increases and with P/P^* becoming zero at the intersection of the curves with the horizontal axis ω/ω^* (point B) when $r/L = 0.57$ as shown in figure 2(e). Notice that point C for $r/L = 0$ in figure 2(a) is also the peak of the curve corresponding to $P_f/P_0 = 1$with a value of $P/P^* = 6.50$.

Figures 3(a-f) show the variation of P/P^* with the ratio P_f / P_0 for different values of ω/ω^*. Note that the curve corresponding to the static case (i.e. $\omega/\omega^* = 0$) remains unchanged for any value of r/L. This curve is identical to that presented recently by [16] in terms of effective length factor K.

Figures 3(a-d) indicate that for the curves corresponding to $\omega/\omega^* = 2$, the buckling load (or the value of P/P^*) is independent of the ratio P_f / P_0 and remains constant for each value of r/L as follows: $P/P^* = 6.50$, 6.05, 4.70, 1.50 and 0 corresponding to $r/L = 0$, 0.15, 0.30, 0.50 and 0.57. The horizontal lines given by $\omega/\omega^* = 2$ in figures 3(a-d) correspond to point C described previously and shown in figures 2(a-e).

Note that when determining the buckling load P using figures 3(a-d), for a given set values of r/L and P_f / P_0, two different values of P can be obtained for certain ranges of ω/ω^*. For instance when using figure 3(a) for $r/L = 0$ two different values of P can be obtained within the range $0 < \omega/\omega^* < 1$. This range is reduced as r/L increases [see figures 3(b-f)]. For instance, for $r/L = 1$ this range is reduced to $0 < \omega/\omega^* < 0.41$. The maximum points marked as D on the curves within these ranges are of special significance since they represent the values of P_f / P_0 where the two values of the buckling load P are identical to each other (i.e., when the loads corresponding to first and second buckling modes become the same value). Also notice that the value of P at point D is reduced significantly as ω/ω^* or r/L increase.

Figures 3(a-f) show that there are three different ranges of ω/ω^* on the variation of P/P^* with respect to P_f/P_0 for each value of r/L. For instance for $r/L= 0$ [see figure 3(a)] within the first range $0 < \omega/\omega^* < 1$ the axial load of the first buckling mode increases as P_f / P_0 increases; within the second range $1 < \omega/\omega^* < 2$ the axial load of the first buckling mode decreases as P_f / P_0 increases; and finally within the third range $\omega/\omega^* > 2$ the axial load of the first buckling mode increases as P_f / P_0 increases. Note that in the second and third ranges there is a single solution for P/P^* for any value of P_f / P_0. Whereas in the first range of ω/ω^*, there are two solutions for P/P^* within some values of P_f / P_0 as described previously.

Figure 4 shows the variation of the peak values of P/P^* versus r/L when the phenomenon of flutter starts to take place for different values of P_f / P_0. Note that in general the critical load at flutter decreases as r/L increases, particularly within the range $0 < r/L < 0.5$ and for large values of P_f / P_0. The presence of the gravity load reduces the peak values of P/P^* within the range $0 < r/L < 0.125$ but alleviates the negative effects of the rotational inertia of the member making the curves in figure 4 less steep. For example when comparing the curves corresponding to $P_f / P_0 = 1.01$ and $P_f / P_0 = \infty$, the presence of the gravity load increases significantly the peak value of P at which flutter occurs for values of $r/L > 0.2$. Therefore, the effects of the gravity load on the dynamic stability of the columns of figures 1(a) and (b) are coupled together with the translational and rotational inertias of the column.

Summary and conclusions

The effects of an end gravity force, translational and rotational inertias along the member on the stability of Reut and Beck columns were presented and discussed using the dynamic formulation. The proposed method and eigenvalue equations are general capturing the static buckling (or divergence) as well as the dynamic instability ("flutter") of slender cantilever columns and subjected to any combination of gravity and non-conservative (fixed-line or follower) axial forces applied at the free end.

Analytical results obtained from the two cases presented (Reut and Beck columns) indicate that: 1) the characteristic equations that include the effects of an end gravity force, translational and rotational inertias of Reut and Beck columns are identical to each other; 2) the dynamic method, as proposed herein, gives the correct solution to any combinations of gravity and non-conservative forces. The dynamic method also captures the limit on the range of applicability of the Euler's method; 3) the transition from static instability (zero frequency) to dynamic instability occurs when $P_f / P_0 = 1$ and the critical loads corresponding to the first and second static buckling mode become identical to each other; and 4) flutter starts to take place when the follower axial load P_f is larger than the gravity load P_0 (i.e. $P_f / P_0 > 1.0$) and when frequencies corresponding to the first and second modes of vibration of the column become identical. Important features of the effects of end gravity force, translational and rotational inertias on the stability of Reut and Beck columns were fully discussed herein.

Acknowledgments

The research presented in this paper was carried out at the National University of Colombia, Structural Stability Group (GES) of the School of Mines at Medellin.

References

1. V. Bolotin. *Non-conservative Problems of the Theory of Elastic Stability*. 1st Ed. The Macmillan Company. New York, USA. 1963. pp. 234.
2. Y. Panovko, I. Gubanova. *Stability and Oscillations of Elastic Systems: Paradoxes, Fallacies, and New Concepts*. 1st ed. Ed. Springer. New York, USA. 1965. pp. 291.
3. V. Feodosyev. *Selected Problems and Questions in Strength of Materials*. Ed. MIR Publishers. Moscow, Russian. 1977. pp. 265-269.
4. M. Langthjem, Y. Sugiyama. "Dynamic stability of columns subjected to follower loads: a survey". *J. of Sound and Vibration*. Vol. 238. 2000. pp. 809-851.
5. Y. Sugiyama, S. Ryu, M. Langthjem. "Beck's column as the ugly duckling". *J. of Sound and Vibration*. Vol. 254. 2002. pp. 407-410.
6. I. Elishakoff. "Controversy associated with the so-called "follower forces": critical overview". *Applied Mechanics Reviews*. Vol. 58. 2005. pp. 117-142.
7. Y. Sugiyama, K. Katayama, S. Kinoi. "Flutter of cantilevered column under rocket thrust." *J. of Aerospace Engineering ASCE*. Vol. 8. 1995. pp. 9-15.
8. S. Ryu, Y. Sugiyama. "Computational dynamics approach to the effect of damping on stability of a cantilevered column subjected to a follower force". *Computers and Structures*. Vol. 81. 2003. pp. 265-271.
9. L. Kwasniewski. "Numerical verification of post-critical Beck's column behavior". *International J. of Non-Linear Mechanics*. Vol. 45. 2010. pp. 242-255.
10. K. Sato. "Instability of a clamped-elastically restrained Timoshenko column carrying a tip load subjected to a follower force". *J. of Sound and Vibration*. Vol. 194. 1996. pp. 623-630.
11. Q. Zuo, H. Schreyer. "Flutter and divergence instability of nonconservative beams and plates". *International J. of Solids and Structures*. Vol. 33. 1996. pp. 1355-1367.
12. W. Glabisz. "Vibration and stability of a beam with elastic supports and concentrated masses under conservative and nonconservative forces". *Computers and Structures*. Vol. 70. 1999. pp. 305-313.
13. I. Elishakoff, N. Impollonia. "Does a partial elastic foundation increase the flutter velocity of a pipe conveying fluid?". *J. of Applied Mechanics. ASME*. Vol. 68. 2001. pp. 206-212.

14. A. Kounadis. "Nonclassical stability problems: Instability of slender tubes under pressure". *J. of Aerospace Engineering. ASCE.* Vol. 14. 2001. pp. 6-11.

15. S. Andersen, J. Thomsen. "Post-critical behavior of Beck's column with a tip mass". *International J. of Non-Linear Mechanics.* Vol. 37. 2002. pp. 135-151.

16. B. Rao, G. Rao. "Post-critical behavior of Euler and Beck columns resting on an elastic foundation". *J. of Sound and Vibration.* Vol. 276. 2004. pp. 1150-1158.

17. F. Detinko. "Lumped damping and stability of Beck column with a tip mass". *International J. of Solids and Structures.* Vol. 40. 2003. pp. 4479-4486.

18. E. Viola, A. Marzani. "Crack effect on dynamic stability of beams under conservative and non-conservative forces". *Engineering Fracture Mechanics.* Vol. 71. 2004. pp. 699-718.

19. J. Aristizabal. "Static stability of beam-columns under combined conservative and nonconservative end forces: effects of semirigid connections". *J. of Engineering Mechanics. ASCE.* Vol. 131. 2005. pp. 473-484.

20. J. Hernandez, J. Aristizabal. "Static and dynamic stability of an elastically restrained Beck column with an attached end mass". *J. of Sound and Vibration.* Vol. 312. 2008. pp. 789-800.

21. D. Zapata, L. Arboleda, J. Aristizabal. "Static stability formulas of a weakened Timoshenko column: effects of shear deformations". *J. of Engineering Mechanics. ASCE.* Vol. 136. 2010. pp. 1528-1536.

22. R. Clough, J. Penzien. *Dynamics of Structures.* 2nd Ed. McGraw – Hill Book Co. New York, USA. 1993. pp. 783

23. A. Chopra. *Dynamics of Structures: Theory and Applications to Earthquake Engineering.* 2nd ed. Prentice Hall. New Jersey, USA. 2000. pp. 844 .

24. S. Timoshenko, J. Gere. *Theory of Elastic Stability*. Engineering Societies Monographs. 2nd ed. Ed. McGraw-Hill Book Company. New York, USA. 1961. pp. 55-59.